Measurements of Electron Energy Distribution on Electron Cyclotron Resonance Plasma Operated with Hydrogen Gas

L. N. Mishra and Å. Fredriksen
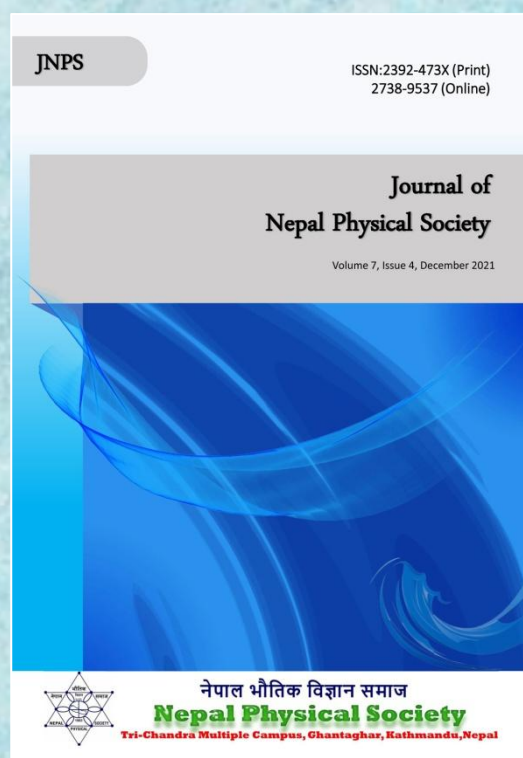
Measurements of Electron Energy Distribution on Electron Cyclotron Resonance Plasma Operated with Hydrogen Gas

L. N. Mishra[1, *] and Å. Fredriksen[2]
[1]Department of Physics, Patan Multiple Campus, Tribhuvan University
[2]Dep. Physics, Faculty of Science, University of Tromsø, N-9037 Tromsø, Norway.
[*]Corresponding Email: lekha.mishra@pmc.tu.edu.np

ABSTRACT

This article deals with the production of electron cyclotron resonance hydrogen plasma in a closed gas chamber called Menja device. For this purpose, 2.45 GHz frequency and various power i.e. 0 - 500 W are employed. The flow of hydrogen gas is controlled manually with the range $1.5 - 10$ sccm maintaining pressure range $10^{-5} - 10^{-4}$ mbar. The Langmuir probe technique is used to drag the electrons and ions by biasing the probe positively and negatively to study the key parameters such as ion saturation current, floating potential, plasma potential, electron temperature and plasma density. Besides these, to obtain information on electron energies and their interaction with plasma, the electron energy distribution function (EEDF) has been studied with the help of 2nd derivative of current obtained from the differentiator. For this purpose, an analogue differentiation circuit was built and tested.

Keywords: Gas chamber, probe, radio frequency, plasma potential.

INTRODUCTION

Nowadays, production of plasma and its applications in different fields such as medicine, agriculture, industry, plasma synthesis and plasma processing are of keen interest for the many researchers. They are being involved on it to innovate the new different techniques to produce the plasma where electron cyclotron resonance is one of them and it is widely used in the plasma processing for industrial applications such as etching [1- 4], thin film deposition [5 -10] and chemical plasma process [11, 12]. Another interesting and important parameter is electron energy distribution function (EEDF) which gives real information about the bombardment of electrons to the wall of the chamber. Not only this but also, it provides the information about the tail of high energetic electrons. Hence, EEDF must be studied. Keeping a view on its importance, many researchers are involved in it to study its mechanism. A key feature of EEDF is that it can be easily computed from the second derivative of the voltage - current characteristics of the Langmuir probe. The relation of EEDF versus probe bias $\mathbf{V_p}$ can be written as [13]

$$f(\varepsilon) = \frac{4}{A_p e^2} \sqrt{\frac{m_e V}{2e}} \frac{d^2 I}{dV_p{}^2} \tag{1}$$

where, I and V_p are the collector current and bias voltage of the probe. A_p is the probe surface area and V is the probe potential relative to plasma potential.

So, simply EEDF is the second derivative of the Langmuir probe characteristics in the range of probe and plasma potential i.e. where $\mathbf{V_p}$ is the probe potential and $\mathbf{V_s}$ the plasma potential.

The electron density can be obtained by integrating the EEDF as

$$n_e = \int_0^\infty f(\varepsilon) \mathrm{d}\varepsilon \tag{2}$$

Furthermore, effective temperature of electron will be

$$\langle T_{eff} \rangle = \frac{2}{3} \langle \varepsilon \rangle \tag{3}$$

There are three different methods to measure the electron energy distribution functions viz., (i)

graphical double differentiation, (ii) recording of the second harmonic direct current of a small ac signal on the probe, and (iii) operating the probe with linear voltage signals and carrying out differentiation with resistance – capacitance (RC) networks or with operational amplifiers [14]. In our case, we have chosen the direct differentiation of probe current with operational amplifiers, so called analogue differentiation circuit, since the graphical method yields the increased noise levels and that of the second harmonic method is quite complicated circuit arrangement.

In this paper, we report the EEDF from the second derivative of I-V characteristics of the Langmuir probe using an analogue differentiation circuit. For this purpose, an analogue differentiation circuit was built and tested.
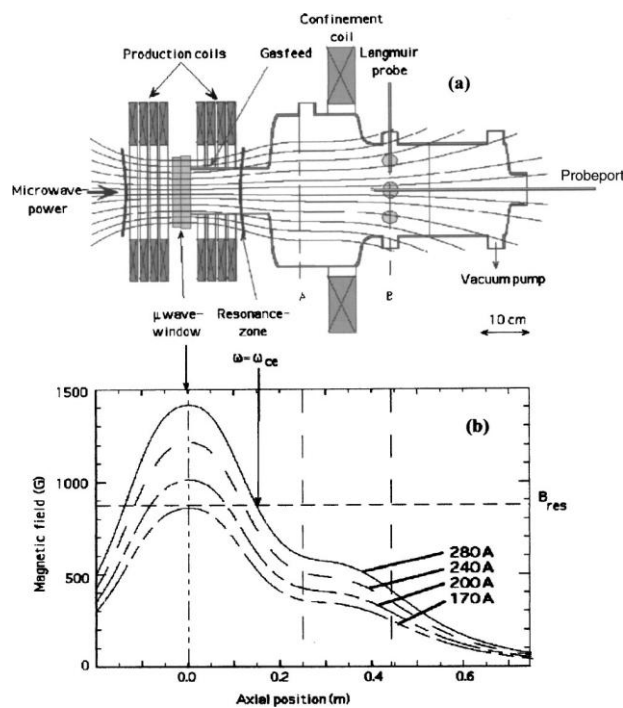
EXPERIMENTAL SETUP

Fig. 1: Experimental arrangement setup (a) and its magnetic field configuration (b) [15].

The experimental arrangement for the experimental study of electron energy distribution on electron resonance plasma operated with hydrogen gas is shown as in FIG. (1). It consists of a cylindrical stainless steel vacuum chamber having 0.85 m length where a magnetic field is produced by passing current from 0 - 230 A on the coils. It is divided into three main parts namely production part, downstream part and processing part. The

resonance zone occurs in the production part which has a small diameter. It is followed by downstream and processing parts. The details about this experimental arrangement could be found in reference to Aanesland et al [15].

The gas chamber is evacuated by Turbo-molecular pump backed with a rotary pump keeping base pressure 10^{-7}mbar. Hydrogen gas is fed through an inlet close to the microwave window. The experiment is carried out within the pressure range from $10^{-5} - 10^{-4}$ mbar keeping gas flow rate 1.25 – 10 sccm. The Langmuir probe is located on a radial port 45 cm from the microwave window. The pressure is recorded using a capacitance manometer and maintained by a feedback loop to an automatic valve on the gas inlet. The gas flow is controlled by using a gas flow meter. The operating gas pressure is optimized by feeding the hydrogen gas in a proper flow rate for achieving good reproduction of the plasma.

Microwaves are produced by an Astex A – 5000 microwave power generator, which delivers power of 500 W at a frequency of 2.45 GHz. Rectangular transverse electric E_{10} waves are fed

into the chamber via a 10 mm thick rectangular quartz window 32×72 mm^2. Two sets of four coils supply the resonant magnetic field in a divergent field configuration, while an extra coil provides improved plasma confinement. The microwave introduction window is placed at the maximum of the magnetic field to protect the window against damage due to strong sputtering. The microwaves propagate through a decreasing magnetic field until they are absorbed by the resonance at the electron cyclotron frequency, where the symbols carry usual meanings. At the resonance condition, the magnetic field is 875 G. The position of the resonance is set by the coil current, and can be located between the microwave window and the end of the production part.

Special care is taken while inserting the probe into the plasma. The probe surface is heated for a while for cleaning purposes under electron bombardment before taking the data. The probe circuit included the grounded chamber wall as a reference, so the plasma potential is obtained with respect to the chamber wall. The probe bias voltage is swept from -40 V to +40 V and probe current is fed to the input of the differentiator. After then, first and second derivatives from the differentiator were recorded by 4 channel data storable Tektronix DPO 4104 digital Oscilloscope. These recorded data were transferred to a personal computer for further analysis.

The movable cylindrical Langmuir probe is inserted into the plasma from a later port of the stainless - steel processing chamber, and it is positioned perpendicularly to the magnetic field, and can be moved in the radial direction. The thin wire probe tip is made of tungsten with 10 mm length and 0.5 mm diameter. The collision-less conditions of a cylindrical Langmuir probe in magnetized plasma is described as a function of four parameters, i.e. the electron free mean path, the probe radius r_p, the plasma Debye length and the Larmor radius, where $l_e \gg r_p \gg l_D$ and $r_L \gg r_p$. The plasma Debye length is given by the formula and the mean Larmor radius for electrons having a Maxwellian energy distribution is.

At the typical operating pressure of our experiments, corresponding to the low-pressure case, the electron mean free path is longer than 10 mm, the Debye length is » 1 mm and the Larmor radius is » 10.0 mm for electrons. To a good approximation, the influence of magnetic field on the probe voltage – current characteristics can be neglected [16].

RESULTS AND DISCUSSIONS

When the magnetic field reaches 875 G, resonance occurs called electron cyclotron resonance. In this case, gas discharge takes place. Hence, the presence of a magnetic field plays an important role and it can affect the probe characteristics because charged particles move along or across the magnetic field lines. A movable single Langmuir probe is placed perpendicular to the magnetic field so that the electron temperature, plasma density, and plasma potential can be measured. For this purpose, stable plasma was established using the best operating condition maintaining pressure $10^{-5} – 10^{-4}$ mbar, gas flow rate 1.25 – 10 sccm and power 500 W. Keeping these parameters constant, we changed the magnetic field by varying the current through the magnetic coils from 170 to 230 A. When current flows 220 to 230 A through the coils, the glow fills entire the discharge chamber and seems optically stable. This is the diffuse discharge mode at which all the data were obtained. Again, when current reduces from 220 to 200 A, the discharge is unstable and flickers, then suddenly contracts toward the symmetry axis. But, the discharge becomes contracted, stable, and the glow when coil current falls to 188 A. This is the contracted discharge mode. From 180 to 170 A, the discharge again becomes noisy, and the glow intensity is quite low.
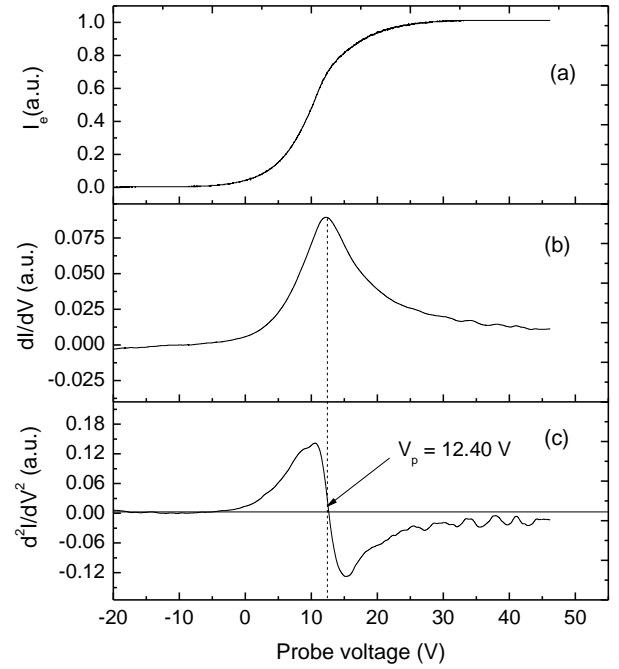

Fig. 2: Typical I-V characteristics (a), its first derivative (b) and second derivative (c) obtained by differentiator at the centre of processing chamber keeping the input microwave power 500 W, coil current for magnetic field 220 A and gas pressure 2.1 x 10^{-4} mbar.

Figure 2 (a), 2 (b) and 2 (c) show the typical I – V characteristics, its first and second derivatives obtained with differentiators. For this case, we employed a Langmuir probe at the center of the processing chamber keeping the input power 500 W with coil current for magnetic field 220 A and gas pressure 2.1 x 10^{-4} mbar with gas flow rate 8 sccm. The zero-crossing crossing point of the second derivative or maxima of the first derivative of the probe current with probe voltages gives the plasma potential. We found the same plasma potential in both cases. The second derivative is further used to obtain the EEDF according to equation (1).

Figure 3 (a), 3(b) and 3 (c) show the variation of plasma density, electron temperature and plasma potential with radial positions at various gas pressure 1.4 x 10^{-4} mbar, 2.1 x 10^{-4} mbar at constant coil current 220 A obtained with a Langmuir probe keeping gas flow at 3 sccm, 8 sccm and forward power 500 W respectively. It is found that the plasma density, electron temperature and plasma potential decrease as the position of the probe gradually moves away from the center of the processing part. In the same system, nitrogen plasma was characterized by Toader et al [17] in two discharge modes, i.e., constricted mode for I_{coil}

> 188 A, and diffuse mode for I_{coil} > 220 A. They also reported the instability of plasma in the magnetic field transition region where 190 A < I_{coil} < 220 A, and for I_{coil} < 180 A and no measurements were made. In the case of the diffuse mode, the plasma density was found to be constant up to 4 cm. The radial variation of the electron temperature for nitrogen plasma is completely different behavior compared to hydrogen plasma. They found the almost same plasma potential along the entire radial position whereas a small potential gradient is observed beyond 5 cm in the case of hydrogen plasma.
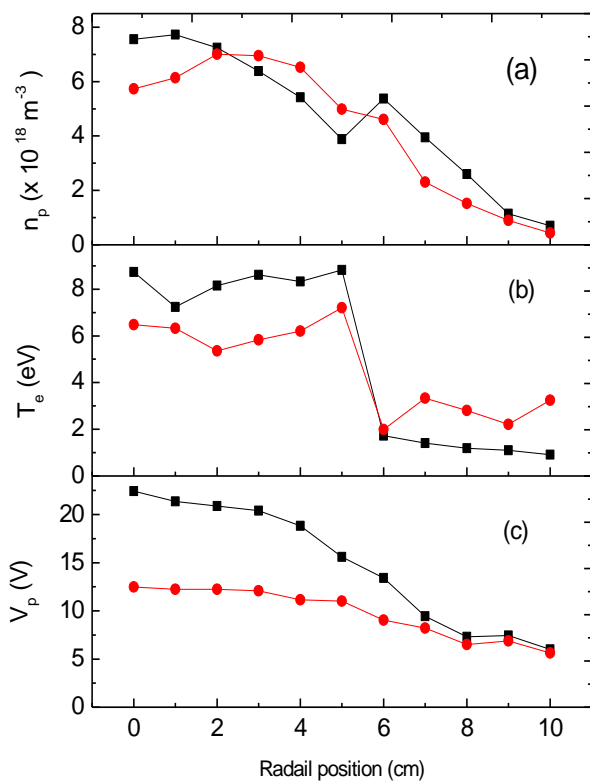

Fig. 3: Radial profiles of plasma density (a) and electron temperature (b) at pressure 1. 4 x 10^{-4} and 2.1 x 10^{-4} mbar with gas flow rate 3 and 8 sccm respectively.

Figure 4(a), 4 (b) and 4(c) show the typical plasma density, electron temperature and plasma potential as a function of working gas pressure. It is found that the plasma density, electron temperature and the plasma potential decrease as the gas pressure increases. It is due to the neutral particle depletion. It was observed by Tynan [18] that below 1.33 x 10^{-5} bar the neutral depletion is proportional to the gas pressure and above 1.33 x 10^{-5} bar the depletion is inversely proportional to the gas pressure.
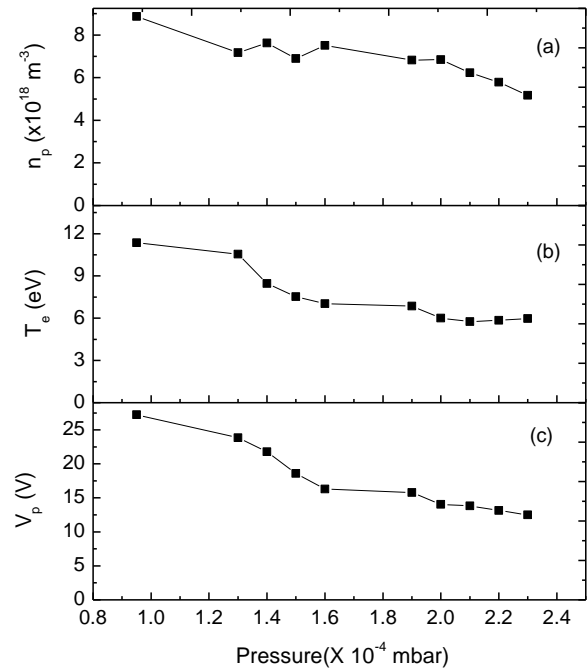

Fig. 4: Variation of plasma density (a), electron temperature (b) and plasma potential as a function of gas pressure.
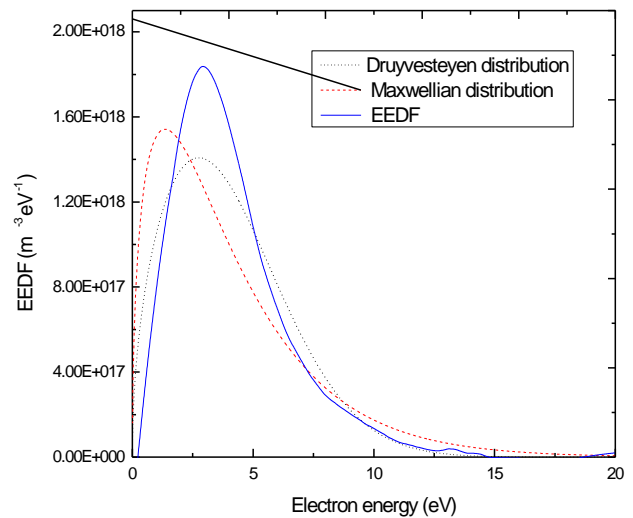

Fig. 5: Typical profiles of Druyvesteyen distribution (dot line), Maxwellian distribution (dash line) and experimental EEDF (solid line) at 4 cm from the processing part keeping pressure 2.1 x 10^{-4} mbar, microwave power 500 W and coil current 220 A respectively.

Figure 5 shows typical profiles of theoretical Druyvesteyn distribution (dot line), Maxwellian distribution (dash line) and experimental EEDF (solid line) at 4 cm from the processing part keeping pressure 2.1 x 10^{-4} mbar, microwave power 500 W and coil current 220 A respectively. The

same plasma parameters viz. plasma density and electron temperature obtained from integration methods using equations (2) and (3) are used to plot the theoretical distributions for the comparison. It is seen that the distribution is fairly Maxwellian. This evolution may be due to the electron- electron collision. In our experiment, plasma density is so high that the electron – electron collision dominates the electron – neutral collision which enhances the distribution as Maxwellian. We employed the following equations [19] for theoretical plots of electron distributions.

$$f_m(\varepsilon) = \frac{2n\varepsilon^{1/2}}{\sqrt{\pi}T_e^{3/2}} exp\left(\frac{-\varepsilon}{T_e}\right) \tag{4}$$

and

$$f_D(\varepsilon) = \frac{1.04n\varepsilon^{1/2}}{E_{av}^{3/2}} exp\left(\frac{-0.55\varepsilon^2}{\varepsilon_{av}^2}\right) \tag{5}$$

where n is the plasma density, ε the electron energy, T_e the electron temperature and ε_{av} the average energy.

In this case, the probe bias voltage is swept from -40 V to + 40 V and all signals were recorded by a storage oscilloscope. The second derivatives are obtained as averages over 512 single measurements each.

CONCLUSIONS

In this work, electron cyclotron resonance plasma has been characterized under the influence of coil current, input power and gas pressure. The radial profile of plasma potential, electron temperature, plasma density has been depicted in a graph with the variation of those mentioned parameters. It is found that the consistent results of plasma potentials have been obtained from both the zero-crossing crossing point of the second derivative or maxima of first derivative of the probe current with probe voltages. The influence of gas pressure on different plasma parameters viz. plasma density, electron temperature and plasma potential has been studied in diffuse discharge mode. It is found that the magnitude of plasma parameters decreases as gas pressure increases. The evolution of electron energy distribution explains how the electrons spread in the vicinity of plasma. It is revealed that the majority of electrons are residing in the low-energy group and those of small populations are residing in the high-energy group. It is seen that the distribution is fairly Maxwellian at all radial points except center.

REFERENCES

[1] Coburn, J. W. and Winters, H. F. *Journal of Vacuum Science and Technology,* **16**: 391 (1979).

[2] Cardinaud, C.; Peignon, M. C. and Tessier, P. Y. *Applied Surface Science* **164:** 72 (2000).

[3] Donnelly, V. M. and Kornblit, A. *Journal of Vacuum Science and Technology A: Vacuum-Surface and Films* **31**: 050825 (2013).

[4] Mogab, C. *Journal of the Electrochemical Society,* **124**: 1262 (1977).

[5] Kemell, M.; Ritala, M. and Leskela, M. *Critical Reviews in Solid-State and Material Science,* **30**: 1 (2005).

[6] Ling, M. M. and Bao, Z. *Chemistry of Materials* **16:** 4824 (2004).

[7] Hunt, A.; Carter, W. and Cochran, J. *Applied Physics Letters* **63:** 266 (1993).

[8] Martin, P. *Journal of Material Science* **21**: 1 (1986).

[9] Hao, X.; Zhang, X. and Lei, L. *Carbon* **47**: 153 (2009).

[10] Sui, S.; Ma, L. and Zhai, Y. *Journal of Power Sources* **196**: 5416 (2011).

[11] Morfill, G.; Kong, M. G. and Zimmermann. *New Journal of Physics* **11:** 115011 (2009).

[12] Davoodbasha, M.; Lee, S. Y.; Kim, S. C. and Kim, J. W. *RSC Advances* **5:** 35052 (2015).

[13] Druyvesteyn, M. J. *Zeitchrift Fur Physic* **64:** 781 (1930).

[14] Nordlund, D. and Breaux, O. *Rev. Sci. Instrum.* **43:** 248 (1972).

[15] Aanesland, A. and Fredriksen, A. *J. Vac. Sci. Technol.* **19:** 2446 (2001).

[16] Richards, S. L. F,; Lloyyd, G. J. and Jones, R. P. *Journal of Physics E: Scientific Instruments* **5:** 595 (1972).

[17] Toader, E.; Fredriksen, A. and Aanesland, A. *Rev. Sci. Instrum.* **74:** 3279 (2003).

[18] Tynan, G. R. *J. Appl. Phys.* **86:** 5356 (1999).

[19] Godyak, V. A. *Plasma - Surface Interaction and Processing of Materials*, Springer, 95-134 (1990).